Jens D. M. Rademacher[1]
Weierstrass Institute for Applied Analysis and Stochastics,
10117 Berlin,
Germany

Ralf W. Wittenberg
Department of Mathematics,
Simon Fraser University,
Burnaby, BC V5A 1S6,
Canada
e-mail: ralf@sfu.ca

Viscous Shocks in the Destabilized Kuramoto-Sivashinsky Equation

We study stationary periodic solutions of the Kuramoto-Sivashinsky (KS) model for complex spatio-temporal dynamics in the presence of an additional linear destabilizing term. In particular, we show the phase space origins of the previously observed stationary "viscous shocks" and related solutions. These arise in a reversible four-dimensional dynamical system as perturbed heteroclinic connections whose tails are joined through a reinjection mechanism due to the linear term. We present numerical evidence that the transition to the KS limit contains a rich bifurcation structure even within the class of stationary reversible solutions. [DOI: 10.1115/1.2338656]

1 Introduction

Nonlinear spatially extended dynamical systems with many degrees of freedom and displaying complex spatial and temporal dynamics and pattern formation are ubiquitous in scientific and engineering applications [1]. The understanding of typical features of such complex and chaotic dynamics has been greatly advanced by the study of canonical models. The Kuramoto-Sivashinsky (KS) equation

$$u_t + u_{xxxx} + u_{xx} + uu_x = 0 \tag{1}$$

has been the subject of extensive study in recent decades as a prototypical example of spatio-temporal chaos (STC) in one space dimension. Originally derived in the context of plasma instabilities [2], flame front propagation [3] and phase turbulence in reaction-diffusion systems [4], this model has been recognized as a generic model for long-wave primary instabilities in the presence of appropriate symmetries [5], in particular spatial and temporal translation invariance, the odd symmetry (parity) $u(x,t)\to -u(-x,t)$, and Galilean invariance. Indeed, the role of the KS equation as a modulation equation for spatially periodic solutions in a reaction-diffusion system has been confirmed through a recent proof [6] of closeness of corresponding solutions. On sufficiently large L-periodic domains, the nonlinear interaction of $O(L/2\pi)$ linearly unstable Fourier modes gives rise to complex dynamics of Eq. (1) in which the long-wave modes act as a "heat bath," driving the chaotic dynamics of the most energetic modes at length scales $O(2\pi)$, so that upon damping or removal of the large-scale modes, the dynamics settles down to a regular roll solution [7,8].

1.1 Stationary Solutions of KS Equation. The understanding of the complex dynamics and intricate bifurcation picture of Eq. (1) for varying domain sizes L begins with the (mostly unstable) stationary and traveling solutions. Since Eq. (1) with $u_t=0$ has a first integral (using $uu_x=(u^2/2)_x$), these may be studied as L-periodic solutions of a third-order ordinary differential equation (ODE), and extensive investigations have revealed a rich structure of odd and asymmetric solutions [9–12].

In particular, the "roll" solutions (also called "cellular" states or Turing patterns) form the backbone to the KS spatial structure, and they have been studied in some detail [13]: the N-modal states have periodicity L/N, lie on the branch bifurcating from the trivial solution at $L=N\cdot 2\pi$, and can be constructed via weakly nonlinear analysis using a Fourier expansion in multiples of the fundamental wave number $2\pi N/L$.

Of particular interest to our work on a modified KS equation are certain stationary spatially odd periodic solutions which consist of periodically matched so-called regular (or monotonic) and oscillatory shocks, as in Fig. 1. Such solutions, their bifurcations, and relations to cells have been studied, for instance, in Refs. [10,14]; they form a solitary wave train from periodically concatenated perturbations of "solitary waves" (homoclinic orbits) such as constructed asymptotically in Ref. [15]. Due to the phase space geometry of these solutions (see Fig. 1(*b*)), we shall refer to them as "bubbles."

1.2 The dKS Equation. We consider the destabilized Kuramoto-Sivashinsky (dKS) equation [16]

$$u_t + u_{xxxx} + \beta u_{xx} + uu_x = \alpha u \tag{2}$$

restricting ourselves to the (invariant) subspace of zero-mean solutions. For $\alpha=0$ and $\beta\neq 0$, Eq. (2) is (a rescaling of) the Kuramoto-Sivashinsky Eq. (1). We will typically consider (following Ref. [16]) $\beta=2$, in which case Eq. (2) may be written in the form $u_t=-(1+\partial_x^2)^2u+(\alpha+1)u-uu_x$; in this form, the role of the term $(\alpha+1)u$ in destabilizing the zero state becomes apparent. However, we retain the freedom to set the parameter β to 0, as the shock-like stationary solutions of Eq. (2) that arise for $\alpha>0$ are robust in this limit. The additional linear term in Eq. (2) breaks the Galilean invariance for $\alpha\neq 0$, and as such (for $\beta=2$ and $-1<\alpha<0$) has been studied in pattern formation and surface growth contexts; see [5,16]. The αu term vertically shifts the linear dispersion relation

$$\lambda = -k^4 + \beta k^2 + \alpha \tag{3}$$

for perturbations from the trivial state, and thus effectively damps (for $\alpha<0$) or drives (for $\alpha>0$) the long-wave modes. The effect on the dynamics is thus as for numerical experiments in which the large-scale modes in KS were suppressed or driven excessively [7,8]: For sufficiently small $\alpha+1>0$, the STC decays and the dynamics settle down to the regular roll state, while for $\alpha>0$ sufficiently large, solutions display rapidly traveling structures and shock-like features. The understanding of STC in the KS equation is thus advanced by studying the transition $\alpha\to 0$, which for $\alpha<0$ occurs via "spatio-temporal intermittency" [17].

1.3 Viscous Shocks. Motivated by the observation in [16] that for sufficiently large α, attracting shock-like odd solutions such as that in Fig. 2 have been observed in L-periodic simula-

[1]Current address: C.W.I. Centrum voor Wiskunde en Informatica, Kruislaan 413, 1098 SJ Amsterdam, The Netherlands.

Contributed by the Design Engineering Division of ASME for publication in the JOURNAL OF COMPUTATIONAL AND NONLINEAR DYNAMICS. Manuscript received December 11, 2005; final manuscript received March 29, 2006. Review conducted by Harry Dankowicz.

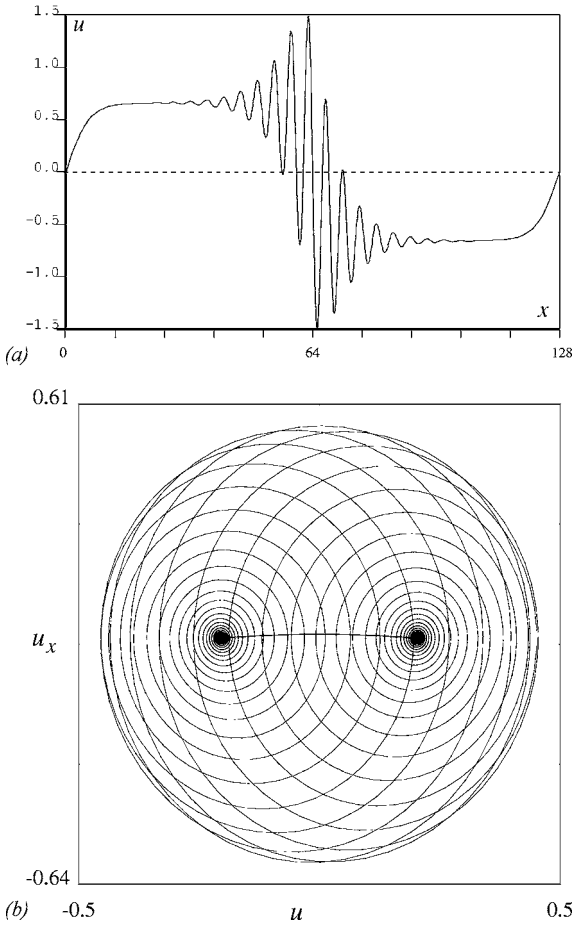

Fig. 1 (*a*) An odd bubble solution for the KS equation ($\alpha=0$) with period $L=128$; (*b*) the (u,u_x) projection of another bubble solution with more oscillations

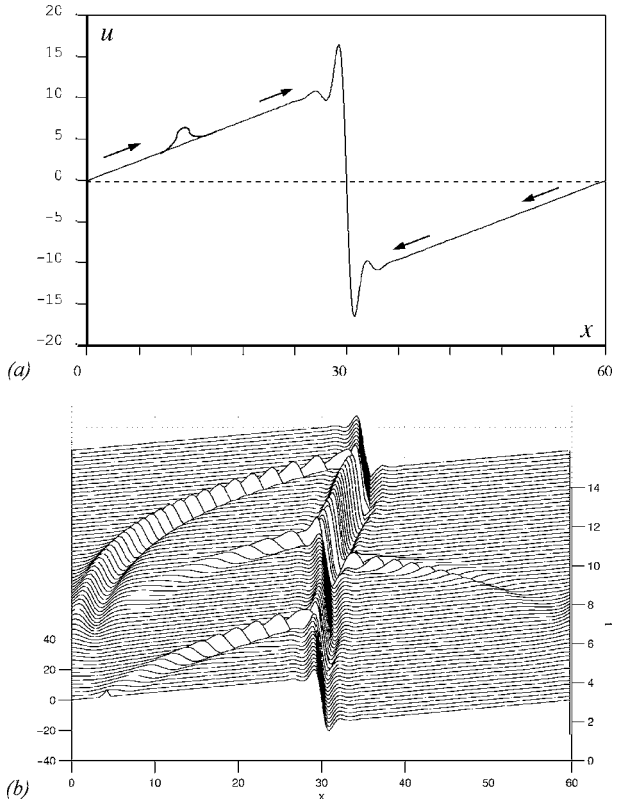

Fig. 3 (*a*) Schematic depiction of direction of transport of localized perturbations along the tail of a viscous shock. (*b*) Time evolution of the dKS equation for $L=60$, $\alpha=0.5$; initial condition is a viscous shock with a small Gaussian perturbation near $x=4$. Note the accelerated transport near the interface.

tions of the partial differential equation (PDE) (2), in the present work we concentrate on certain stationary solutions for $\alpha>0$, which satisfy

$$u_{xxxx}+\beta u_{xx}+uu_x=\alpha u \tag{4}$$

The "tails" of these solutions are close to spatially linear solutions with slope α: indeed Eq. (4) has the exact solution $u(x)=\alpha x$. The shock-like interface arises when u is constrained to be periodic, and we shall see below that as $L\to\infty$, the interface scales to a jump for $L^{-1}u(Lx)$; thus we refer to these solutions as *viscous shocks*.

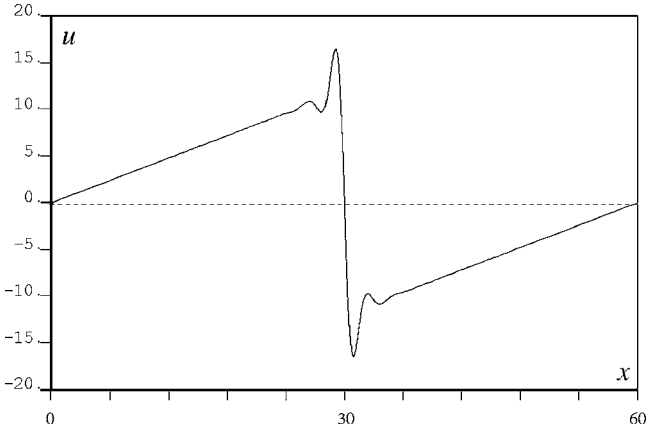

Fig. 2 Odd viscous shock of period $L=60$ for $\alpha=0.4$

The origin of viscous shocks as L-periodic orbits in the four-dimensional phase space associated with Eq. (4) is discussed at some depth in Sec. 4: The emergence of viscous shocks is due to a reinjection mechanism for $\alpha>0$ by which certain heteroclinic solutions become periodic. Precisely the same effect, but in a much simpler context, occurs in the so-called Burgers-Sivashinsky equation [18], and for illustrative purposes we discuss it in some detail in Sec. 3.

In the limit of unbounded period, viscous shocks exist up to $\alpha=0$ and converge to fronts in the KS equation. As the integration constant for the stationary KS equation becomes unbounded, the aforementioned bubbles converge to the same fronts [9,10]. It might thus seem natural that viscous shocks bifurcate from bubbles as α increases from 0. In Sec. 5 we present numerical evidence that viscous shocks for large α are indeed path connected to bubbles in the (α,L)-parameter space. However, it appears that for fixed period L, there is no connection in α from $\alpha=0$ to viscous shocks for large α; instead, as α decreases viscous shocks either destabilize in a Hopf bifurcation or cease to exist at a fold point at some $\alpha>0$.

1.4 Viscous Shocks as a Source-Sink Compound. For the PDE (2), one may heuristically view viscous shocks as a robust connection between a "source" at the center (zero intercept) of the tail and a "sink" at the shock interface, because localized perturbations between the two zero intercepts are transported towards the shock interface, as indicated by the cartoon in Fig. 3(*a*). Indeed, the variation $w=u-\alpha x$ about the linear part in the profile (choosing $x=0$ at the center of the linear tail) satisfies

$$w_t + \alpha x w_x = -(w_{xxxx} + \beta w_{xx} + w w_x)$$

For small, smooth initial $w(\cdot,0)$ localized near any $x \neq 0$ we expect that the right-hand side of the above equation remains much smaller than $\alpha x w_x$ due to smoothness, at least for a short time. Neglecting the right-hand side during this time, for $\alpha > 0$ the coefficient αx of the convection term is positive for positive x, implying transport away from a "source" at $x=0$ where $u=0$, $u_x \approx \alpha$, to the right for positive x and to the left for negative x. Since the transport depends on the u elevation, one may interpret it as a remnant of the Galilean invariance of the KS equation ($\alpha = 0$). In fact, the characteristics of the hyperbolic part on the left-hand side are $(t, x_0 e^{\alpha t})$, which implies a spreading of the perturbations from the center and an accelerated transport towards the shock interface.

This effect is observed in numerical simulations of the dKS Eq. (2), such as that plotted in Fig. 3(*b*), in which the (stable) viscous shock for $L=60$, $\alpha=0.5$ initially receives a small Gaussian perturbation along the tail to the right of $u=0$. Note the direction of transport of perturbations of the linear tail, to the right for $u>0$ and to the left for $u<0$, and the distinct acceleration nearing the interface as predicted; the final stationary state is a translation of the original viscous shock. For smaller α, for which the viscous shock is no longer an attractor, similar persistent wave transport towards the (remnants of the) interface is characteristic of the transition to STC as α decreases to 0.

1.5 Scaling of Bounds on the Attractor. The existence of large amplitude viscous shock solutions is of particular interest in the context of the scaling of rigorous bounds on the dKS attractor (see Refs. [16,19] for discussions). All numerically computed or analytically approximated known solutions of the KS Eq. (1) on bounded domains of length L appear to have amplitude $|u(x,t)|$ uniformly bounded independent of L; but while partial proofs of this are known, notably the result of Michelson [9] of a uniform bound for all stationary solutions, a general L_∞ bound for Eq. (1) has remained elusive. Analytical estimates typically proceed via the L_2 norm, defined by the energy $\|u\|_2^2 = \int_0^L u^2 dx$; uniform boundedness of u would imply $\limsup_{t\to\infty} \|u\|_2 \leq CL^{1/2}$, or that the energy density is finite. This scaling appears natural in the spatio-temporally chaotic KS limit, as it is consistent with decay of spatial correlations and extensivity, that is, local dynamics independent of system size and unaffected by distant boundaries.

The asymptotic scaling of the viscous shock solutions of Eq. (2), as observed numerically [16] and shown in Sec. 4 below, shows that the dKS equation does *not* have extensive dynamics: For any $\alpha > 0$, as the period $L \to \infty$ the L_∞ and L_2 norms scale as $\|u\|_\infty = O(\alpha L)$, $\|u\|_2 = O(\alpha L^{3/2})$, which implies that the best possible bound on the KS absorbing ball using a method valid also for $\alpha > 0$ should be $\limsup_{t\to\infty} \|u\|_2 \leq CL^{3/2}$. By an improved construction of the gauge function ϕ, Bronski and Gambill [19] have recently shown that the exponent 3/2 can indeed be achieved using a Lyapunov-type argument to proving bounds, and is optimal for such an approach. Thus for the dKS equation we have the bound $\limsup_{t\to\infty} \|u\|_2 \leq C(\alpha) L^{3/2}$, and the viscous shock solution saturates the bound. (The best current estimate for the absorbing ball of the KS equation for $\alpha=0$ is $\limsup_{t\to\infty} \|u\|_2 = o(L^{3/2})$, using a method, inapplicable for $\alpha > 0$, of treating the KS solution at large scales like an entropy solution of Burgers' equation [20]).

2 Phase Space Formulation for Stationary Solutions

In preparation for studying the stationary solutions of the dKS equation, we rewrite Eq. (4) as a first-order system:

$$u_x = u_1$$

$$u_{1,x} = u_2$$

$$u_{2,x} = u_3$$

$$u_{3,x} = -\beta u_2 - u u_1 + \alpha u \tag{5}$$

or, more briefly, $U_x = F(U;\alpha)$, where we denote $U = (U_0, U_1, U_2, U_3) = (u, u_1, u_2, u_3)$. The system (5) is measure preserving, because the trace of its linearization vanishes. The odd symmetry $u \to -u$, $x \to -x$ of Eq. (4) yields the reversible symmetry of Eq. (5) with respect to the reflection $R(u,u_1,u_2,u_3) = (-u,u_1,-u_2,u_3)$, which has the symmetry plane $S_R = \{(0,a,0,b) \,|\, a,b \in \mathbb{R}\}$, orthogonal to the flow. We refer to solutions that are symmetric with respect to the reflection as *reversible*.

The single odd linear solution αx of Eq. (4) plays an important role, and we view it as an invariant reversible one-dimensional manifold $\ell_\alpha = \{(a,\alpha,0,0) \,|\, a \in \mathbb{R}\}$ in the phase space of Eq. (5); note that ℓ_0 is a line of equilibria.

In anticipation of the stability considerations in Sec. 5, we introduce the linearization of Eq. (2) about a solution $u(x)$,

$$\mathcal{L}(u)v = v_{xxxx} + \beta v_{xx} + v u_x + u v_x - \alpha v \tag{6}$$

The eigenvalue problem $\lambda v + \mathcal{L}(u)v = 0$ with appropriate boundary conditions (possibly at infinity) determines the spectrum of $\mathcal{L}(u)$ (also referred to as the spectrum of u) for the PDE (2) and thereby the stability of a stationary solution u. We recast this eigenvalue problem as a first-order linear non-autonomous ODE of the form $V_x = B(x;\lambda)V$, where $B(x;\lambda) = A(u(x), u_x(x), \lambda)$ with

$$A(u,u_1,\lambda) := \partial_U F(U;\alpha) - \lambda \begin{pmatrix} 0 & 0 & 0 & 0 \\ 0 & 0 & 0 & 0 \\ 0 & 0 & 0 & 0 \\ 1 & 0 & 0 & 0 \end{pmatrix} = \begin{pmatrix} 0 & 1 & 0 & 0 \\ 0 & 0 & 1 & 0 \\ 0 & 0 & 0 & 1 \\ \alpha - u_1 - \lambda & -u & -\beta & 0 \end{pmatrix} \tag{7}$$

Note that for $\lambda = 0$ this is the linearization of the spatial dynamics (5) in u.

For $\alpha \neq 0$ the unique spatially uniform steady state $u(x)=0$ of Eq. (2) corresponds to the unique equilibrium $U=(0,0,0,0)$ in Eq. (5). The eigenvalues of the linearization $A(0,0,0)$ about the trivial state are

$$\pm\nu_\pm(\alpha) = \pm\sqrt{-\frac{\beta}{2} \pm \sqrt{\frac{\beta^2}{4} + \alpha}}$$

whose real and imaginary parts are monotone functions of α. In particular, $\nu_-(0) = \sqrt{\beta}\,\mathrm{i}$, $\nu_+(0) = 0$, and for $\beta = 2$ we have $\nu_\pm(-1) = \mathrm{i}$. Hence, for $\beta = 2$, as α varies from 0 to -1 all resonances occur, which has consequences for the bifurcation of periodic orbits [10].

However, our interest is the destabilized regime $\alpha > 0$, where the aforementioned viscous shocks shown in Fig. 2 were found. In this regime, $A(0,0,0)$ has a pair of complex conjugate pure imaginary eigenvalues and two non-vanishing real eigenvalues with same absolute value but opposite signs. Hence, using Devaney's reversible Lyapunov center theorem for reversible equilibria [21] (Theorem 8.1) and the formulas for $\nu_\pm(\alpha)$, we can immediately deduce the existence of a family of periodic orbits in a manifold tangent to the center eigenspace: For any $\alpha > 0$ and $\beta \geq 0$, system Eq. (5) possesses a two-dimensional invariant manifold containing the origin which consists of a nested one-parameter family of reversible periodic solutions, whose period tends to $2\pi/|\nu_-(\alpha)|$ as the initial condition approaches the origin.

These symmetric periodic orbits, similar to Turing patterns, are *roll* (or cellular) solutions, which a priori have small amplitude, but numerically continue to solutions with relatively large amplitude; examples of such patterns (with fixed period L and varying

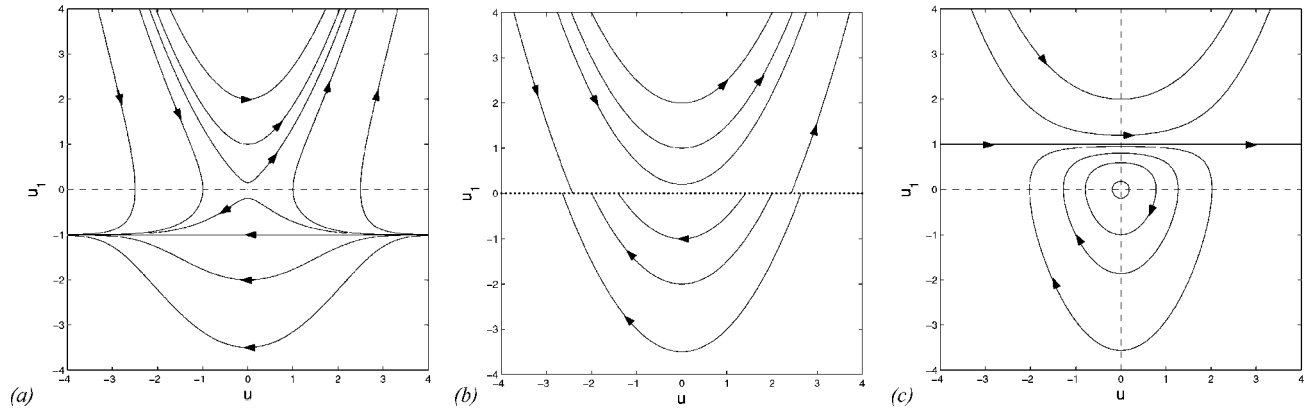

Fig. 4 Phase portraits for stationary solutions of the Burgers-Sivashinsky system (9) for (*a*) $\alpha=-1$, (*b*) $\alpha=0$, and (*c*) $\alpha=1$

α) are shown in Fig. 12 below. The wavelength of these stationary patterns is set by the condition $\lambda=0$, where the spectrum (3) of the trivial solution $u\equiv 0$ crosses the imaginary axis at non-zero wave number $k^2=\beta/2+\sqrt{\beta^2/4+\alpha}$.

3 Burgers-Sivashinsky Equation

To illustrate the phase space analysis for the investigation of steady states of Eq. (2) and for comparison, we consider the simpler destabilized Burgers or so-called "Burgers-Sivashinsky" (B-S) equation [18,19]

$$u_t - u_{xx} + uu_x = \alpha u \tag{8}$$

For $\alpha>0$, this equation has similar viscous shock-like solutions, consisting of an outer linear solution and a steep inner transition layer which is near a heteroclinic connection.

The first-order system for stationary solutions of Eq. (8) is

$$u_x = u_1$$

$$u_{1,x} = uu_1 - \alpha u \tag{9}$$

This system is reversible with symmetry line $m_R=\{u=0\}$, and has the same linear solution $u=\alpha x$ as Eq. (4), whose orbit in Eq. (9) we denote by ℓ_α as well. Since the phase space is only two dimensional, the analysis is simple, and we can give a complete characterization of stationary solutions. We first show that for $\alpha\leq 0$ there are no non-trivial periodic solutions, and then consider $\alpha>0$.

For $\alpha<0$, elementary phase plane analysis shows that the unique equilibrium at the origin $u=0$ is the only bounded stationary solution of Eq. (8) (see Fig. 4(*a*)). For $\alpha=0$, the line $\ell_0=\{u_1=0\}$ consists of fixed points which we denote by $u=\pm c$, $c\geq 0$. Orbits in the half-plane $u_1>0$ are unbounded, but the region $u_1<0$ is fibered by spatially heteroclinic odd orbits $h_c(x)$, as shown in Fig. 4(*b*). These are the only non-trivial bounded stationary solutions and satisfy $h_{c,x}=1/2(h_c^2-c^2)$, $h_c(\mp\infty)=\pm c$. Choosing the spatial origin so that $h_c(0)=0$, we find $c=\sqrt{-2h_{c,x}(0)}$, and hence upon integration the explicit formula $h_c(x)=-c\tanh(cx/2)$.

3.1 Viscous Shocks in the B-S Equation. We may summarize the behavior for $\alpha>0$ as follows:

THEOREM 1. *For any $\alpha>0$ the flow of Eq. (9) maps $m_R\cap\{u_1<0\}$ to $m_R\cap\{0<u_1<\alpha\}$ reversing the order of the u_1 component. The nontrivial, bounded stationary solutions of Eq. (8) are given by a one-parameter family $u_c(x)$ of nested spatially periodic odd solutions, parametrized by $c=\sqrt{-2u_{c,x}(0)}\in\mathbb{R}^+$. Letting $L=L(\alpha,c)$ be the period of such a solution, the slope $u_x=u_1$ increases monotonically for $x\in[0,L/2]$, and $L\to 2\pi/\sqrt{\alpha}$ as $c\to 0$. As $c\to\infty$, for fixed x the solutions $u_c(x)$ converge locally uniformly to $h_c(x)$, and $u_c(\cdot+L/2)$ converge locally uniformly to ℓ_α. In this limit, we can estimate the period as $L=2c/\alpha(1+o(1)_{c\to\infty})$, the amplitude as $\alpha L+o(1)_{c\to\infty}<2\max\{u(x)\,|\,x\in[0,L]\}<\alpha L$, and $u_{c,x}(L/2)=\alpha+O(e^{-c^2/2\alpha})_{c\to\infty}$.*

Proof. We prove the above statements by using reversibility and phase space methods to identify the periodic solutions, emphasizing a readily generalized geometric approach; the corresponding phase portrait for $\alpha=1$ is shown in Fig. 4(*c*).

For $\alpha>0$, the unique fixed point is again at the origin $(u,u_1)=(0,0)$. The invariant line ℓ_α and the region above it contain no bounded solutions, since for $u_x=u_1\geq\alpha$, u is monotonically increasing.

We parametrize the solutions $U_c=U(x)=(u,u_1)$ of Eq. (9) below ℓ_α by $c\geq 0$, so that $U(0)=(0,-c^2/2)$ is the initial condition on the symmetry line $m_R\cap\{u_1<0\}$. For small positive x, U enters the sector $\{u<0,u_1<0\}$. By Eq. (9) u is decreasing, and u_1 increasing in this sector, so that the orbit U must intersect $\{u_1=0\}$ at $u=-u^*(c,\alpha)$, $x=x_1$ (with $u^*>0$) to enter the sector $A=\{u<0,\ 0<u_1<\alpha\}$, remaining entirely below the invariant line ℓ_α. Since u and u_1 are increasing in A, we deduce that U must intersect the symmetry line m_R for $u_1>0$ at some $x_*=x_*(c,\alpha)$. Since $u_x=u_1<\alpha$ in region A, we have $u(x)<-u^*+\alpha(x-x_1)$ in this region, so that the "time" to traverse this region is $x_*-x_1>u^*/\alpha$. By reversibility, we conclude that U is a closed orbit of period $2x_*=L=L(c,\alpha)$. Hence the phase plane below ℓ_α is fibered by reversible periodic orbits, for which more negative $u_1(0)=-c^2/2$ are mapped to larger $u(x_*)=u(L/2)$, that is, closer to ℓ_α, and $u_1=u_x$ increases monotonically for $x\in(0,L/2)$.

The eigenvalues of the linearization of Eq. (9) about the trivial solution $(0,0)$ are $\pm\sqrt{\alpha}i$, which immediately implies the period in the limit $c\to 0^+$ of small-amplitude oscillations.

The large-amplitude limit of stationary solutions of long period may be studied by rescaling with a scale parameter $\delta>0$: setting $x=\delta y$, $v=\delta u$, the function $v(y)$ satisfies Eq. (9) with α replaced by $\delta^2\alpha$, and with $v_y(0)=-(\delta c)^2/2=-\tilde{c}^2/2$. Thus for fixed $v_y(0)<0$, the convergence of $v(y)$ to the heteroclinic $h_{\tilde{c}}$ as $\delta\to 0$ is apparent. Since $c=\delta^{-1}\sqrt{-2v_y(0)}$, this corresponds for $u(x)$ to the limit $c\to\infty$, in which u converges to the heteroclinic $h_c=-c\tanh(cx/2)$. Since $h_c(\infty)=-c$, to leading order the amplitude and period are found from $u^*\sim c$ and $x_*\sim L/2\sim c/\alpha$, so $u^*\sim\alpha L/2$ (note that the contribution to the period from the heteroclinic is lower order, $x_1/x^*=o(1)_{c\to\infty}$).

The behavior near ℓ_α is best analyzed by moving the spatial origin to the intersection $m_R\cap\{u_1>0\}$, and considering the variation about ℓ_α via $w(x)=\alpha x-u(L/2+x)$, so that $w(0)=0$,

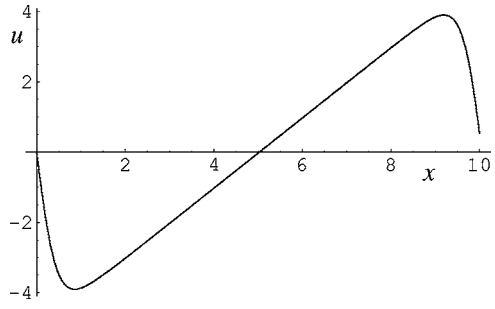

Fig. 5 Profile of a "viscous shock" of the Burgers-Sivashinsky Eq. (8) with $\alpha=1$

$w_x(0)=\alpha-u_1(L/2)>0$. Then (by reversibility) the repulsion rate of w_x from $w_x(0)$ as x increases corresponds to the attraction of u to ℓ_α in region A. The solution w satisfies $w_{xx}-\alpha x w_x=-w w_x$, which we integrate via variation of constants to

$$w_x(x)=w_x(0)e^{\alpha x^2/2}-\int_0^x e^{\alpha(x^2-s^2)/2}w(s)w_x(s)ds$$

Hence on a linear level, neglecting the last term, the growth of w_x in x, and hence the attraction of $\ell_\alpha\cap\{u<0\}$ in the transverse direction in $(x-L/2)$, is super exponential. Since the "time" that u spends in A (until $w_x=\alpha$) is $x_*-x_1=c/\alpha+o(1)_{c\to\infty}$, we find $w_x(0)=O(e^{-\alpha(x_*-x_1)^2/2})=O(e^{-c^2/2\alpha})$, so the midpoint slope, at the intercept with $m_R\cap\{u_1>0\}$, is $u_x=\alpha+O(e^{-c^2/2\alpha})_{c\to\infty}$ □

In this particular two-dimensional system, we may confirm the above conclusions directly from the first integral $u_1+\alpha\log|\alpha-u_1|-u^2/2=K$, where $K=-c^2/2+\alpha\log\alpha(1+c^2/2\alpha)$ for the solution through $(0,-c^2/2)$. Writing $w_1=1-u_1/\alpha$ this becomes $w_1-\log w_1+u^2/2\alpha=1+c^2/2\alpha-\log(1+c^2/2\alpha)$. Straightforward expansions for $c^2/2\alpha\gg1$ show that the intercepts with m_R are at $w_1=1+c^2/2\alpha$ (that is, $u_1=-c^2/2$), and $u_1=\alpha(1-w_1^*)$ for $w_1^*=(1+c^2/2\alpha)e^{-(1+c^2/2\alpha)}+O((w_1^*)^2)$; and that the maximum value of $|u|$ (at $u_1=0$) is $u^*=\max_x|u|=c(1-\alpha/c^2\log c^2/2\alpha+O(c^{-4}))$. In fact, we have $w_1e^{-w_1}=(1+c^2/2\alpha)e^{-1+(u^2-c^2)/2\alpha}$, so for small $|u|$, $w_1\sim w_1^*e^{u^2/2\alpha}$. Since near $x=L/2$, $u\sim\alpha(x-L/2)$, we have $w_1\sim e^{\alpha(x-L/2)^2/2}$, verifying the super-exponential growth.

Remark. Many of the results about the stationary solutions of Eq. (8) are contained in Ref. [18], where the argument proceeds via matched asymptotics. The purpose here is to illustrate the approach by phase space analysis and the role of ℓ_α in organizing the "viscous shocks" of Eq. (8) for $\alpha>0$ only.

We emphasize that these bounded solutions, which are similar to the viscous shocks in Eq. (2), do not oscillate in space. A typical such orbit for $\alpha=1$ is shown in Fig. 5. In Sec. 4 we show that the viscous shocks for the four-dimensional ODE (5) arise due to a similar phase space geometry, but oscillate near ℓ_α.

Goodman [18] investigated stability in the B-S equation, and in particular argued that Eq. (8) in the space of periodic mean zero solutions has a gradient structure, which excludes temporal oscillations and chaotic behavior; and that the stable stationary solutions are those whose minimal period is the domain length.

For the dKS Eq. (2), both the stability and the classification of steady states are more complicated, and we present numerical results for the bifurcations and spectrum of viscous shocks in Sec. 5. Indeed, the linearization of Eq. (8) in a viscous shock has a real spectrum, while some viscous shocks in Eq. (2) undergo Hopf bifurcations as α is varied.

4 Existence of Viscous Shocks

By comparison with the B-S Eq. (8), the detection of viscous shocks in the dKS equation is more challenging due to the four-dimensional phase space of Eq. (5). However, the structural similarity is that both equations produce heteroclinic connections in a rescaled limit, and that the flow along the special solution αx provides a re-injection mechanism that perturbs these heteroclinic orbits to periodic ones. The viscous shock solutions are thus constructed as periodic orbits in Eq. (4) by patching together a perturbed heteroclinic orbit with a trajectory near the invariant line ℓ_α.

4.1 Heteroclinic Orbits. We work in coordinates appropriate to the heteroclinic connections. To blow up the inner layer of viscous shocks, we thus rescale Eq. (2) via $x=\delta y$ and balance by $u=\delta^{-3}v$, which upon multiplication with δ^7 yields

$$v_{yyyy}+vv_y=\delta^2(-\beta v_{yy}+\delta^2\alpha v) \tag{10}$$

We consider Eq. (10) in its first-order formulation

$$\begin{aligned} v_y&=v_1\\ v_{1,y}&=v_2\\ v_{2,y}&=v_3\\ v_{3,y}&=-vv_1-\delta^2\beta v_2+\delta^4\alpha v \end{aligned} \tag{11}$$

which has the same reversible symmetry R as Eq. (5), reflection about the symmetry plane S_R, and the invariant line in these coordinates is $\ell_{\delta^4\alpha}=\{(a,\delta^4\alpha,0,0)\,|\,a\in\mathbb{R}\}$.

We begin by studying the unperturbed heteroclinic orbits: For $\delta=0$ Eq. (10) is the integrable equation

$$v_{yyyy}+\frac{1}{2}(v^2)_y=0 \tag{12}$$

or $v_{yyy}+v^2/2=c^2/2$, where c is a constant (nontrivial bounded solutions are found only for positive integration constant). In this case, rescaling via $v=cw$ and $z=(c/2)^{1/3}y$ yields

$$w_{zzz}=1-w^2 \tag{13}$$

Apart from the hyperbolic fixed points at $w_\pm=\pm1$, this equation has a *unique* (up to translation) bounded solution, the heteroclinic orbit $h(z)$ [22]. This orbit lies in the transverse intersection of the two-dimensional stable and unstable manifolds of the equilibria $w_-=-1$ and $w_+=+1$, respectively, and intersects the symmetry plane $w=w_{zz}=0$ with negative slope w_z. We can choose the origin $z=0$ so that h is a reversible orbit, with $h(\pm\infty)=\mp1$, $h(0)=h_{zz}(0)=0$, and $h_z(0)<0$; and we define the amplitude of the heteroclinic orbit $h_{\max}=\|h\|_\infty=\max_{z\in\mathbb{R}}|h(z)|>1$.

Returning to the limiting inner Eq. (12), we thus obtain a one-parameter family of reversible heteroclinic orbits $h_c(y)=ch((c/2)^{1/3}y)$, which connect the equilibria $\pm c$; note that $h_{c,yyy}(0)=c^2/2h_{yyy}(0)=c^2/2$. Let $H_c=(h_c,h_{c,y},h_{c,yy},h_{c,yyy})$ denote the solution of the first-order system associated with Eq. (12). Then H_c lies in the transverse intersection of the stable and unstable manifolds $\mathcal{W}^s(-c)$, $\mathcal{W}^u(c)$ of $\pm c$ [9,22]. The unique intersection of the heteroclinic orbit H_c with the symmetry plane S_R is at $z=0$, with $H_c(0)=(0,a(c),0,c^2/2)\in S_R$, where $a(c)=(c^4/2)^{1/3}h_z(0)<0$ for all $c>0$; observe that $a(c)\to-\infty$ as $c\to\infty$, and that the amplitude is $\max_y h_c(y)=ch_{\max}$.

4.2 Invariant Line. Having discussed the unperturbed heteroclinic orbit, we next characterize the invariant line $\ell_{\delta^4\alpha}$ in the rescaled coordinates: *The invariant manifold* $\ell_{\delta^4\alpha}\backslash\{(0,\delta^4\alpha,0,0)\}$ *of* (11) *is normally hyperbolic, that is, the three-dimensional transverse linear flow near* $\ell_{\delta^4\alpha}$ *is hyperbolic away from the symmetry plane* S_R. *For each* $v<0$, *the eigenspaces of the linearization of the transverse flow are transverse to the* v *direction, with*

the transverse eigenvalues consisting of one real unstable eigenvalue and a stable complex conjugate pair of eigenvalues. Moreover, for $v<0$ and any $\delta>0$, the unstable eigenvalue is strictly monotone increasing as v decreases, and the real parts of the stable eigenvalues, which are the leading eigenvalues, are strictly monotone decreasing.

We prove this by linearizing Eq. (11) about $v_1=\delta^4\alpha$, $v_2=v_3=0$ at a fixed v, to find that the linearized matrix $A(v,v_1,0)$ from Eq. (7) takes the α-independent form

$$A_\delta(v):=\begin{pmatrix}0 & 1 & 0 & 0\\ 0 & 0 & 1 & 0\\ 0 & 0 & 0 & 1\\ 0 & -v & -\beta\delta^2 & 0\end{pmatrix}$$

whose characteristic polynomial is $\nu(\nu^3+v+\beta\delta^2\nu)$. In addition to the eigenvalue $\nu=0$, corresponding to the flow along the invariant line, we have three transverse eigenvalues $\nu_j(v)$, $j=0,1,2$. For $\beta\delta^2=0$, these eigenvalues are straightforwardly found as $\nu_j(v)=(-v)^{1/3}e^{2\pi ij/3}$, while for $\beta\delta^2>0$, the roots of the cubic are found using Vieta's substitution $\nu=w-\beta\delta^2/(3w)$, where $w^3=g$ satisfies $g^2+vg-(\beta\delta^2/3)^3=0$; we obtain

$$\nu_j(v)=e^{2\pi ij/3}g^{1/3}-\delta^2e^{-2\pi ij/3}\frac{\beta}{3g^{1/3}} \tag{14}$$

where $g\in\mathbb{R}$ is

$$g=-\frac{v}{2}+\sqrt{\frac{v^2}{4}+\delta^6\frac{\beta^3}{27}}>0$$

We observe that $\nu_0\in\mathbb{R}$, and that $\mathrm{sgn}(\nu_0)=-\mathrm{sgn}(v)$ (since for $\beta\delta^2>0$, we compute $\nu_0\geq 0$ if and only if $g^2\geq(\beta\delta^2/3)^3$, which from the governing quadratic equation for $g>0$ holds if and only if $v\leq 0$). The monotonicity of ν_0 in v is obvious for $\beta\delta^2=0$, and otherwise follows from $dg/dv<0$ and $d\nu_0/dg>0$.

The remaining eigenvalues $\nu_j(v)$, $j=1,2$ are complex conjugate, with real part $\mathrm{Re}(\nu_j)=-\nu_0/2$, from which the stability and monotonicity of the complex eigenvalues follows. Therefore $\ell_{\delta^4\alpha}$ is normally hyperbolic, but not uniformly, because at $S_R\cap\ell_{\delta^4\alpha}=(0,\delta^4\alpha,0,0)$ all eigenvalues lie on the imaginary axis. Since the eigenvalues are distinct, eigenspaces are transverse to each other and the v direction is the kernel.

4.3 Phase Space Origins of Viscous Shock. Having established the properties of the invariant line and the heteroclinic connections, as for the B-S Eq. (9) we can locate viscous shocks as trajectories of Eq. (11) beginning in the symmetry plane S_R which track an unperturbed heteroclinic orbit into the vicinity of the invariant line $\ell_{\delta^4\alpha}$, and are then transported by the flow along this line back into the symmetry plane. However, the analysis is more subtle in this case owing to the higher dimensionality, and as discussed below, we expect that a blow-up analysis will be required to make the following arguments fully rigorous. To ensure proximity to the heteroclinic solutions of Eq. (12), the construction depends on suitable smallness conditions on both $\delta^4\alpha$ and $\delta^2\beta$, which may be combined in a single perturbation parameter, for instance, $\delta^2\beta+\delta^4\alpha$. However, for the sake of clarity we consider fixed, though arbitrary, values $\alpha>0$ and $\beta\geq 0$, and take δ as the perturbation parameter; we observe that all constructed trajectories and manifolds depend smoothly on α, β and δ. For ease of notation we do not distinguish between constants $K>0$, which may be chosen successively smaller.

Let $\Phi_y(U)$ denote the flow of Eq. (11). Taking initial data $U\in S_R$ in the symmetry plane, we let $\mathcal{O}_\pm(U)=\{\Phi_y(U)\mid y\in\mathbb{R}^\pm,|y|\leq\min\{|y|>0\mid\Phi_y(U)\in S_R\}\}$ represent the partial forward or backward orbit under the flow before the next intersection with $S_R=\{v=0,v_2=0\}$. Using reversibility we identify periodic solutions, with period $\tilde{L}$ in y, as orbits beginning in S_R, which again intersect S_R at $y=\tilde{L}/2$.

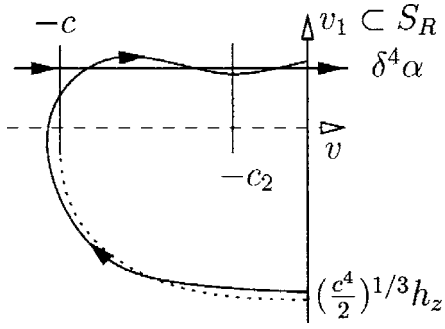

Fig. 6 Sketch of the phase space projected into the (v,v_1) plane for $\delta>0$; note that the v_1 axis lies in S_R. The dashed line is the heteroclinic H_c for $\delta=0$.

First we observe that there are orbits beginning in S_R which closely track an unperturbed heteroclinic orbit and are attracted arbitrarily closely to the invariant line $\ell_{\delta^4\alpha}$. Indeed, consider a compact subinterval $\ell_{\delta^4\alpha}^{c_1,c_2}=\{(v,\delta^4\alpha,0,0)\mid -c_1\leq v\leq -c_2<0\}$ of $\ell_{\delta^4\alpha}$. By our previous calculations the interval of equilibria $\ell_0^{c_1,c_2}$ is normally hyperbolic with combined rate $\kappa_1=\mathrm{Re}(\nu_1(-c_2))>0$, since the real parts of the eigenvalues are monotonic in v. By Fenichel theory [23], (Theorem 9.1), the stable and unstable manifolds are preserved under perturbation, so that there is a $K>0$ such that whenever $0<\delta\leq K$, the orbit segment $\ell_{\delta^4\alpha}^{c_1,c_2}$ has locally (in y) stable and unstable manifolds $\mathcal{W}_\delta^{s/u}$ such that any orbit decays towards or diverges from $\ell_{\delta^4\alpha}^{c_1,c_2}$ with rate at least $\kappa_1/2$, as long as it stays in these manifolds. (In fact, as for the B-S equation we observe that for a viscous shock solution, the attraction towards $\ell_{\delta^4\alpha}$ is super exponential in $y-\tilde{L}/2$.)

We recall that for $\delta=0$ we have a one-parameter family of heteroclinic orbits H_c, so that the stable manifold of $\ell_0^{c_1,c_2}$ transversely intersects S_R with negative v_1 component in a curve $\mathcal{H}$, and an initial condition $H_c(0)=(0,a(c),0,c^2/2)$ in $\mathcal{H}$ approaches the equilibrium at $U_{c,0}^-=(-c,0,0,0)$ for some $c>0$ in an oscillatory manner.

The stable manifold $\mathcal{W}_\delta^s$ converges locally uniformly as $\delta\to 0$ to the stable manifold of $\ell_0^{c_1,c_2}$, and the decay in the stable fibers is exponential, while the distance of the invariant line to the v axis is $\delta^4\alpha$, polynomial in δ. Hence for sufficiently small $K>0$, for $0<\delta\leq K$ the local stable manifold $\mathcal{W}_\delta^s$ intersects S_R in a curve $\mathcal{H}_\delta$, which converges uniformly to a compact subset of $\mathcal{H}$ as $\delta\to 0$. Let $V_{c,\delta}(0)\in S_R$ be an initial condition in $\mathcal{H}_\delta$ which approaches $H_c(0)$ as $\delta\to 0$ for some c, $-c_1\leq -c<-c_2$. Then the trajectory $V_{c,\delta}=\mathcal{O}_+(V_{c,\delta}(0))$ approaches a neighborhood of $U_{c,\delta}^-=(-c,\delta^4\alpha,0,0)$, and thus in particular attains a positive v_1 component. The flow proceeds in the direction of increasing v, and since it maps stable fibers to stable fibers, such a trajectory remains in the stable manifold $\mathcal{W}_\delta^s$, retaining a strictly positive v_1 component and exponentially approaching the invariant line $\ell_{\delta^4\alpha}$. By continuity (possibly for smaller $K>0$) for any $0<\delta\leq K$, such an orbit crosses the section $\{v=0,v_1>0\}$.

We thus now have, for a given sufficiently small $\delta>0$, a one-parameter family of trajectories $V_{c,\delta}$, smoothly parametrized by c, which are initially perturbations of a family of heteroclinic orbits H_c, are attracted to the vicinity of the invariant line $\ell_{\delta^4\alpha}$, and then flow in the direction of increasing v until they cross the hyperplane $\{v=0\}$, as indicated schematically in Fig. 6. To locate a reversible periodic orbit, we now make use of the additional freedom in c to obtain an intersection with the symmetry plane S_R. Let $b_\delta(c)$ be the value of v_2 at the intersection of $V_{c,\delta}$ with the hyperplane $\{v=0\}$; then we require $b_\delta(c)=0$ (this requirement, due to

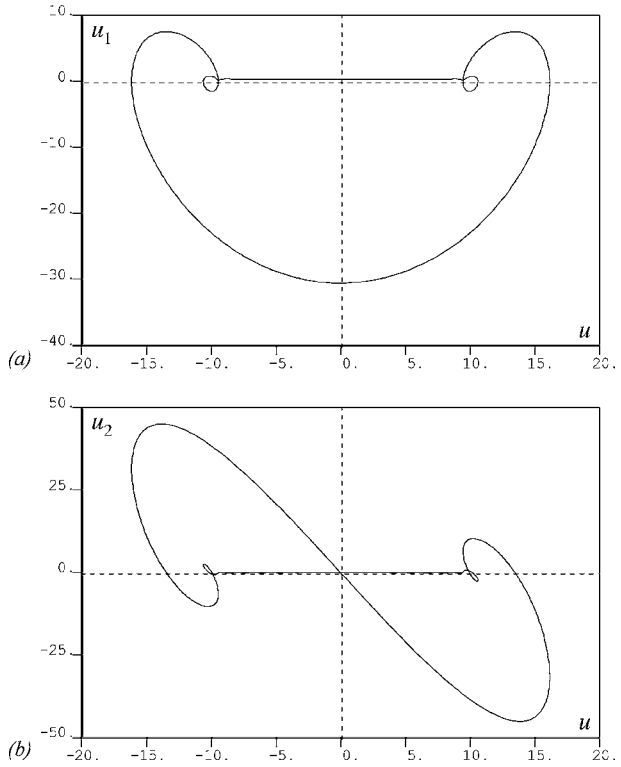

Fig. 7 Phase space projections of the viscous shock from Fig. 2 onto the planes (*a*) (u, u_1) and (*b*) (u, u_2)

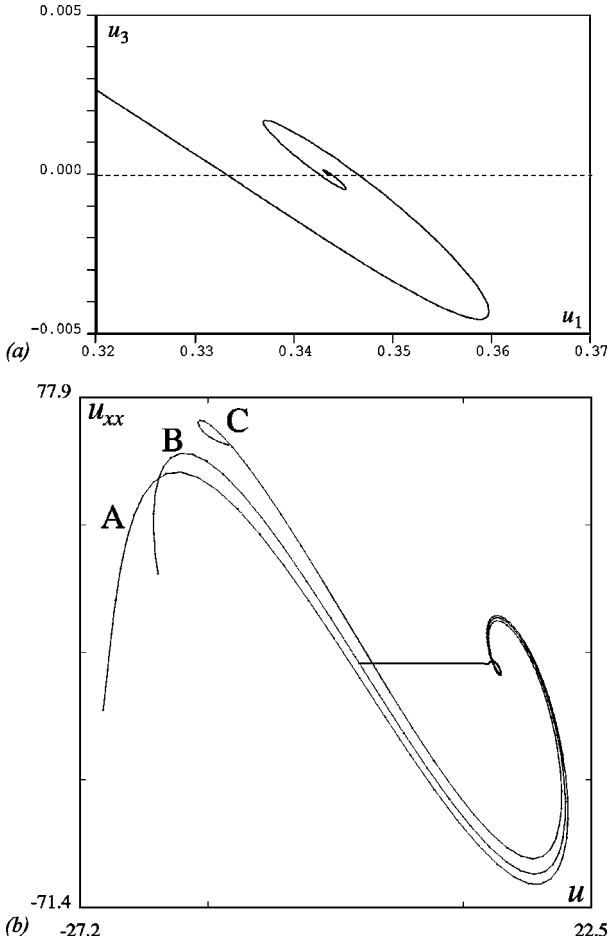

Fig. 8 (*a*) Intersections of viscous shocks with S_R for fixed $\alpha \approx 0.3435$ parametrized by $L \in (40, 62)$. (*b*) Projections to the (u, u_{xx}) plane of trajectories of Eq. (5) with $\alpha = 0.4$ and initial conditions $u = u_{xx} = u_{xxx} = 0$, and A: $u_x = 0.3999999991$ B: $u_x = 0.39999999915$ C: $u_x = 0.3999999992$.

the higher dimensionality of the phase space of Eq. (11), is part of the reason for the additional complexity not present in the two-dimensional B-S problem).

One may argue as follows: the invariant line $\ell_{\delta^4\alpha}$ lies in the plane $\{v_2 = 0, v_3 = 0\}$. By our previous computations, the transverse flow in the local stable manifold is exponentially attracted to $\ell_{\delta^4\alpha}^{c_1,c_2}$ (in fact, for increasing c the trajectory $V_{c,\delta}$ spends longer in the stable fibration, and thus approaches the origin in (v_2, v_3) more closely). Furthermore, the transverse flow is an oscillation, so that the v_2-v_3 projection oscillates in y, hence as a function of distance along $\ell_{\delta^4\alpha}$. Since the distance traveled along $\ell_{\delta^4\alpha}$ increases with c, we expect that $b_\delta(c)$ oscillates about $v_2 = 0$ as a function of c; consequently for sufficiently small δ, there is a $c_* = c_*(\delta, \alpha, \beta)$ so that $b_\delta(c_*) = 0$. This gives us the desired reversible periodic orbit. By construction, this orbit is initially near an unperturbed heteroclinic, and is then exponentially attracted to the invariant line $\ell_{\delta^4\alpha}$, where $v_1 \approx$ constant; so this corresponds to a viscous shock solution, as in Fig. 7. This viscous shock $V_{c_*,\delta}(y)$ in the rescaled variables (corresponding to a viscous shock $U_{c_*,\delta}(x)$ in the original variables) depends smoothly on the parameters δ, α, and β.

We may further verify this phase space picture by looking at the geometry of the intersection of a branch of viscous shocks, obtained by fixing $c_*(\delta, \alpha, \beta)$, with the symmetry plane S_R. For instance, for fixed $\alpha > 0$ and $\beta \geq 0$, decreasing δ increases the length of the flow along $\ell_{\delta^4\alpha}$, and thus increases the period $\tilde{L}$, or L in the original variables (see the discussion on scaling below). Since the transverse flow in the stable manifold of $\ell_{\delta^4\alpha}$ is an oscillation and contraction as a function of distance traveled, we expect the intersection with S_R to spiral in towards $v_1 = \delta^4\alpha$ (that is, $u_1 = \alpha$), $v_3 = 0$ with decreasing δ (or increasing L); this prediction is verified in Fig. 8(*a*).

Numerically, one can most easily locate viscous shocks as attracting stationary solutions of the dKS Eq. (2) for sufficiently large α and L; however, one can also obtain good approximations by a shooting method in Eq. (5) (in the original variables $u(x)$). In this case, it is convenient to reverse the above construction, by starting in S_R near $u_x = \alpha$ and trying to hit $S_R = \{(u, u_{xx}) = (0, 0)\}$ again, since by reversibility such an intersection corresponds to a periodic solution. In Fig. 8(*b*) we plot the results of such a shooting approach for $\alpha = 0.4$, in which we varied the initial $u_1 = u_x$ and considered the projection of the resulting orbits in the (u, u_2) plane. Observe that at the intersection with $u = 0$, trajectories A and C indeed lie on either side of the origin $u_{xx} = 0$, which confirms the existence of a periodic solution (near trajectory B). Note how the presence of an unstable manifold of ℓ_α leads to extreme sensitivity to the initial u_x value.

Remark. The above existence argument for the dKS viscous shocks is not rigorous in its present form, as we only have normal hyperbolicity of the invariant line $\ell_{\delta^4\alpha}$ for $v \neq 0$, not at the intersection with the symmetry plane S_R. Thus we are not a priori guaranteed the desired smoothness of and rates of attraction within the stable manifold $\mathcal{W}_\delta^s$ uniformly up to S_R. (Furthermore, the presence of a two-dimensional transverse unstable manifold $\mathcal{W}_\delta^u$ of $\ell_{\delta^4\alpha}^{c_1,c_2}$—also not present in the B-S equation—implies that great care is needed with continuity arguments based on perturbing the orbits constructed above.)

We expect that by a so-called blow-up analysis it is possible to rigorously prove the existence of viscous shocks and related solutions, as well as their scaling in terms of α and L as discussed below. The blow-up approach to a non-hyperbolic equilibrium

with nilpotent part is a change to spherical coordinates together with a desingularization that renders the non-hyperbolic equilibrium a sphere with several *hyperbolic* equilibria and heteroclinic connections that can be treated classically. It has been used successfully in low ambient dimensions for singularly perturbed problems where the slow manifold is folded at a non-hyperbolic point and transitions between opposing parts produce special solutions; straightening such a one-dimensional fold, one obtains a line of equilibria similar to ℓ_0 (see, for instance, Ref. [24]).

4.4 Scaling of Viscous Shocks. The constructed viscous shock solutions $V_{c_*,\delta}(y)$ approach the vicinity of the invariant line near $v=-c_*$, and then proceed towards S_R with speed $v_1 \sim \delta^4\alpha$, which occurs along a y interval of length $\sim c_*/\delta^4\alpha$. The leading-order estimate of the period in y is thus $\tilde{L} \sim 2c_*/\delta^4\alpha$, while as $\delta \to 0$, the contribution from the flow near the heteroclinic H_{c_*} is of lower order, $O(1)$ in y.

The intersections with the symmetry plane S_R occur for $v_1 \sim \delta^4\alpha$ (with, presumably, exponentially small corrections, as for the B-S equation) along the "linear" part of the viscous shock, and $v_1 \sim a(c_*) = (c_*{}^4/2)^{1/3} h_z(0) < 0$ in the transition layer region. The amplitude of the shock is $\max_{y\in\mathbb{R}} |v| \sim c_* h_{\max} + o(1)_{\delta\to 0}$, which is slightly greater than c_*, the overshoot being due to the heteroclinic orbit.

We hence deduce the scaling of the viscous shock solutions in the original variables, $x=\delta y$ and $u=\delta^{-3}v$. The period L along a branch of viscous shocks (with a particular c_*) satisfies $L=L(\delta,\alpha,\beta)=\delta\tilde{L} \sim \delta \cdot 2c_*/\delta^4\alpha$. Treating the period L as a parameter (which is appropriate as we frequently seek solutions of the PDE on a domain with a given period), and solving for $\delta=\delta(L,\alpha,\beta) \sim (2c_*/\alpha L)^{1/3}$, we observe that each branch of viscous shock solutions is a smooth three-dimensional manifold parametrized by L, α, and β.

The transition layer width due to the heteroclinic, which is $O(1)$ in y, is $O(\delta)=O((\alpha L)^{-1/3})$ in the original x variable, as predicted and observed numerically in Ref. [16] and used for the gauge function construction in Ref. [19]. Further, since $u_1=u_x=\delta^{-4}v_y$, the intersections with the symmetry plane S_R occur with slope $u_x \sim \alpha$ in the outer, linear regime (corresponding to the dominant balance $uu_x \sim \alpha u$ in Eq. (4)) and $u_x \sim (\alpha L/4)^{4/3} h_z(0)$ in the center of the viscous shock. Last, the amplitude is $\|u\|_\infty \sim \frac{h_{\max}}{2}\alpha L$, while the leading contribution to the L_2 norm is due to the outer, linear part, giving $\|u\|_2^2 \sim \alpha^2 L^3/12$, thus confirming the scaling results for $\|u\|_\infty$ and $\|u\|_2$ discussed previously.

The *existence criterion* for these viscous shocks from our approach is (for fixed $\beta \geq 0$) a smallness condition on δ. Since for $\delta \to 0$, $\delta=O((\alpha L)^{-1/3})$, we thus have that

> *there exists a constant K^* such that viscous shocks exists for $\alpha L \geq K^*$*

(The requirement that $\alpha\delta^4$ be sufficiently small leads to an additional criterion that αL^4 be large enough, $\alpha L^4 \geq \tilde{K}^*$, say, which becomes relevant for short-period solutions with large α.) While we have only shown this criterion to be sufficient (not necessary), we thus suspect that the viscous shocks do not bifurcate from $\alpha=0$, that is, from solutions of the KS Eq. (1) with finite period, and this is shown numerically in Sec. 5 below.

5 Numerical Continuation, Stability and Related Solutions

For sufficiently large αL, the above argument indicates that viscous shocks exist, and indeed they are numerically observed to be attracting [16]. Towards seeking to understand the nature of and transitions towards spatio-temporal chaos in the KS Eq. (1), it is of interest to investigate what happens to the viscous shocks as α decreases towards the KS limit $\alpha=0$. In this limit, we know the viscous shocks cease to exist, both by our arguments in Sec. 4 and from the fact that the amplitude of the viscous shocks is proportional to L, while that of stationary KS solutions is uniformly bounded [9] in L; but one might surmise that they are connected in parameter space to some interesting KS solutions. This idea is particularly attractive as the inner layers (in the limit of infinite period L) of viscous shocks in the dKS equation and of fronts in the KS equation are the same, being the heteroclinic connections of Eq. (12) (see [9], Theorem 2.2). It turns out, however, that while viscous shocks are path connected to the KS equation in the (α,L)-parameter plane, there is no direct path connection for fixed α or fixed L.

The full dynamics and bifurcations of the dKS equation in the $\alpha \to 0$ limit are complicated, and we merely summarize here our preliminary investigations of the very restricted case of reversible, stationary solutions. We concentrate on solutions to the boundary-value problem for the system (5) (with $\beta=2$) with boundary conditions $u=u_2=0$ at $x=0, L/2$, which by reversibility are L-periodic stationary solutions of the dKS Eq. (2). We continue these solutions in the parameters α and L using the software package AUTO [25]; the highly accurate numerical method is of predictor-corrector type, incorporating a Newton method and spatial discretization by collocation.

Our main observation is the following: *It appears that for any fixed period L, the continuation of a branch of viscous shocks for decreasing α undergoes a fold at some $\alpha_*(L)>0$; the same holds when α is held fixed and L decreased. The continuation of the set of folds of viscous shocks $\{(\alpha_*(L),L)\} \subset \mathbb{R}^2$ consists of bounded disconnected curves along which the nature of the solutions changes. These curves terminate in cusps at some $\alpha>0$ and roll solutions for some $\alpha<0$, while at $\alpha=0$ the solution is a bubble.*

This observation, consistent with the sufficient (though not necessary) existence criterion for viscous shocks, is supported by the numerical results shown in the figures and discussed below. We plot a typical continuation branch of viscous shocks for fixed period $L=60$ in Fig. 9(*a*); with decreasing α the branch experiences a fold, or saddle node bifurcation, at some $\alpha>0$. In fact, there are regions in the (α,L) plane where many more sheets of stationary solutions coexist, and we plot some such branches in Fig. 9(*b*).

5.1 Reversible Solutions of the dKS Equation. Several different families of reversible periodic solutions are observed along the branches of Fig. 9 and similar bifurcation curves; the main types are shown in Figs. 10–12 (note that by reversibility, we need to show only half of the solution). Since most of these solutions have interfaces similar to that of viscous shocks, we propose a classification of these in terms of the geometry of their tails away from the shock interface:

- **Viscous shocks:** Solutions with the slope of tail near $u_x \approx \alpha$; see two examples in Fig. 10. This family incorporates the viscous shocks for large αL discussed in Sec. 4, and solutions obtained from these by continuing in the (α,L)-parameter plane without passing a fold.
- **Flat shocks:** These solutions have a shock-like interface similar to that of viscous shocks, and a nearly vanishing slope in the tail (with decaying oscillations); see Fig. 11(*a*). Flat shocks come in a family parametrized by the length of the flat region and the length of the region near ℓ_α.
- **Roll shocks:** The oscillatory tails of these solutions are reminiscent of the roll solutions (Turing-like patterns), while their interface is similar to that of viscous shocks; see Fig. 11(*b*). The family of roll shocks is parametrized by the length of the region near a roll pattern, and the amplitude and period of these, as well as by the length of the linear region near ℓ_α. (These are not the oscillatory shocks of the KS Eq. (1), whose *interfaces*, not tails, oscillate [14,15].)

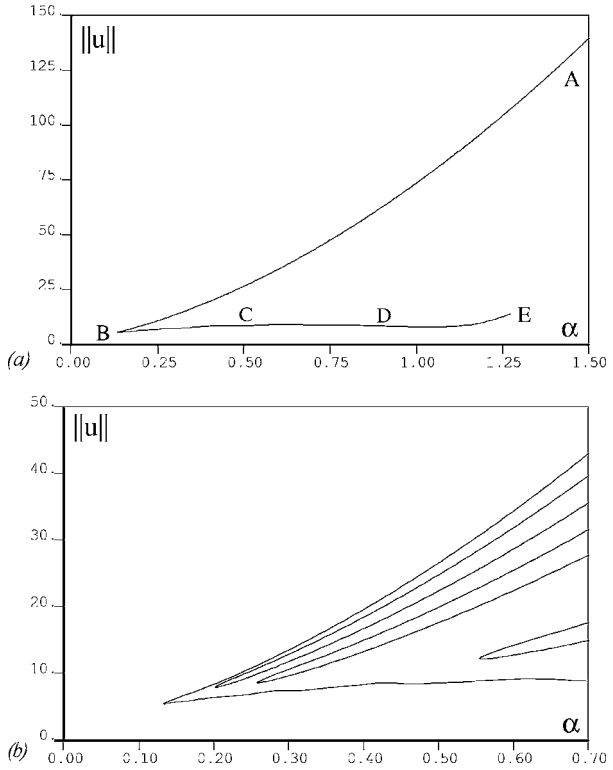

Fig. 9 (*a*) Paths of reversible periodic orbits of period $L=60$, continuing in α; labeled solutions are shown in Figs. 10–12. (*b*) A section through several sheets of shocks for $L=60$. The upper branch is one of viscous shocks, while the shocks on branches with lower amplitude have a longer flat region.

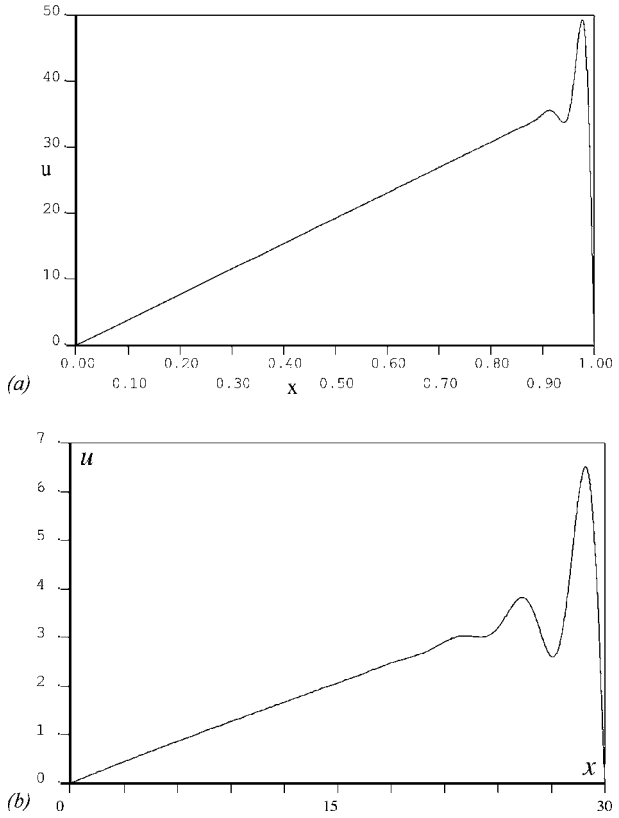

Fig. 10 Viscous shocks: Labeled solutions (*a*) A and (*b*) B from Fig. 9(*a*)

Other solutions observed include the previously discussed roll solutions (parametrized by their amplitude and wave number, which limits to $|\nu_-|$ for small amplitude; see Fig. 12) and bubbles as in Fig. 1.

Regarding the existence of flat and roll shocks, we conjecture the following: *Flat and roll shocks can be constructed similarly to viscous shocks by following the heteroclinic orbits H_c and the reinjection provided by ℓ_α, but leaving the vicinity of ℓ_α in its unstable direction*: *Roll shocks occur near an intersection of the local unstable manifold of ℓ_α for $u<0$ and the stable manifold of the roll solutions discussed in* Sec. 2; *they start in S_R near $\mathcal{H}$, but eventually follow the unstable fiber and remain near the roll for a while before intersecting S_R again. Similarly, flat shocks are near an intersection of the unstable manifold of ℓ_α and the stable manifold of the origin.*

The solutions plotted in Figs. 10 and 11 support this conjecture: these solutions may have an extended region near ℓ_α, but diverge from it before u reaches zero away from the shock interface, and approach either a roll solution or the origin.

5.2 Folds of Viscous Shocks. For sufficiently large αL, we have seen that (for $\beta=2$) there exists a two-parameter family of viscous shocks; we now consider the boundary of this sheet of viscous shocks in (α, L) parameter space. As mentioned above, for typical fixed period this boundary is a fold, and we plot in Fig. 13 the numerical continuation of several such folds in the (α, L) plane. The nature of the solutions along these folds changes with α, eventually terminating in roll solutions for $\alpha \leq 0$, while for $\alpha>0$ the corners of these curves are cusps, where two folds meet. Note that only the components of the fold curves intersecting $\alpha=0$ are relevant to viscous shocks, while beyond the cusps for $\alpha>0$, the observed folds are the boundaries of sheets of flat shocks.

The intersection of these fold curves with $\alpha=0$ shows the path connectedness of dKS viscous shocks and certain bubbles of the KS equation, but in all our computations the branch of a fold at $\alpha=0$ does not connect directly to the sheet of viscous shocks for *fixed L*. Instead, it connects to rolls at $\alpha>0$ via flat and roll shocks. This can be partially understood by the points with horizontal slope in the graph of Fig. 13, for example, at the dashed horizontal line: above the dashed line the fold of viscous shocks is the rightmost one, but below the dashed line it is the leftmost one. Indeed, at the degenerate fold where the curve has vanishing slope, the sheet of viscous shocks touches a sheet of flat shocks and "rips" for increasing period, thus producing another curve of folds. We illustrate this ripping process in Fig. 14, by showing various cross sections at constant L of surfaces of reversible stationary solutions of the dKS equation; in each case solution "A" is connected (for large α and L) to the sheet of viscous shocks, while "B" and "C" connect to flat shocks for increasing α.

Observe the upper envelope of the folds in Fig. 13 (approximately sketched by the thick dotted curve): above and to the right of the envelope—which appears to have the form of a hyperbola—viscous shocks are guaranteed to exist, consistent with the prediction $\alpha L \geq K^*$ previously derived as a sufficient condition for the existence of viscous shocks.

For increasing L the fold curves in Fig. 13 become steeper and move closer to $\alpha=0$, and we conjecture that this scenario repeats further as L increases, consistent with our previous scaling results. Indeed, the dKS Eq. (2) has the scaling symmetry $x \mapsto x/\delta$, $t \mapsto t/\delta^4$, $u \mapsto \delta^3 u$, $\alpha \mapsto \delta^4 \alpha$, $\beta \mapsto \delta^2 \beta$. For $\beta=0$, we thus have exact scaling symmetry in the α-L parameter space, which persists in approximate form for fixed $\beta>0$.

While numerical continuation fails, it appears that the fold curves may connect via small-amplitude rolls for $\alpha<0$ to the trivial solution $u \equiv 0$ at $\alpha=0$. For $\alpha=0$, the fold curves connect to bubble solutions of the KS equation; Fig. 1(*a*) shows one such

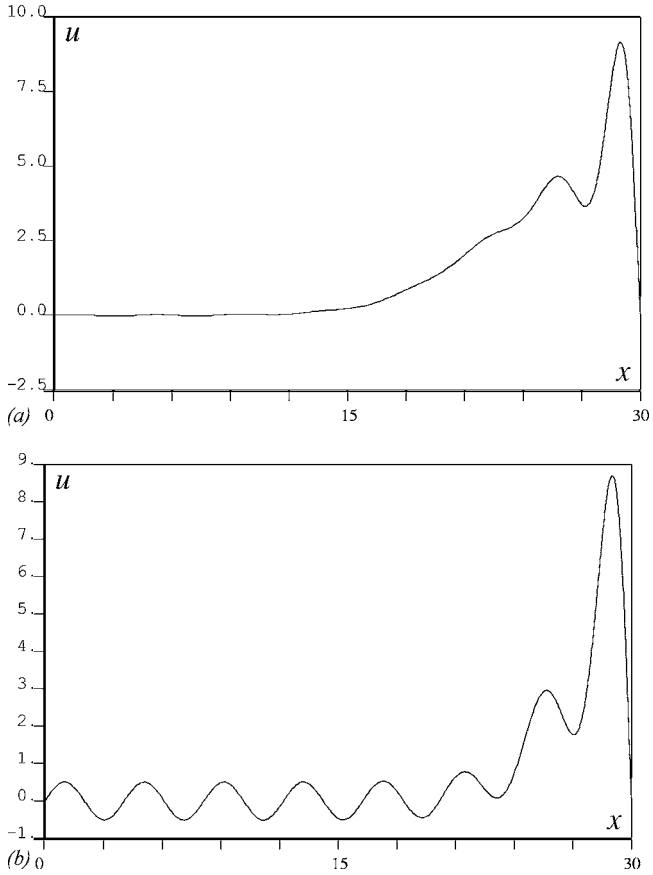

Fig. 11 Flat and roll shocks: (*a*) A flat shock: solution C from Fig. 9(*a*), remaining near ℓ_α for a while; (*b*) a roll shock: solution D from Fig. 9(*a*)

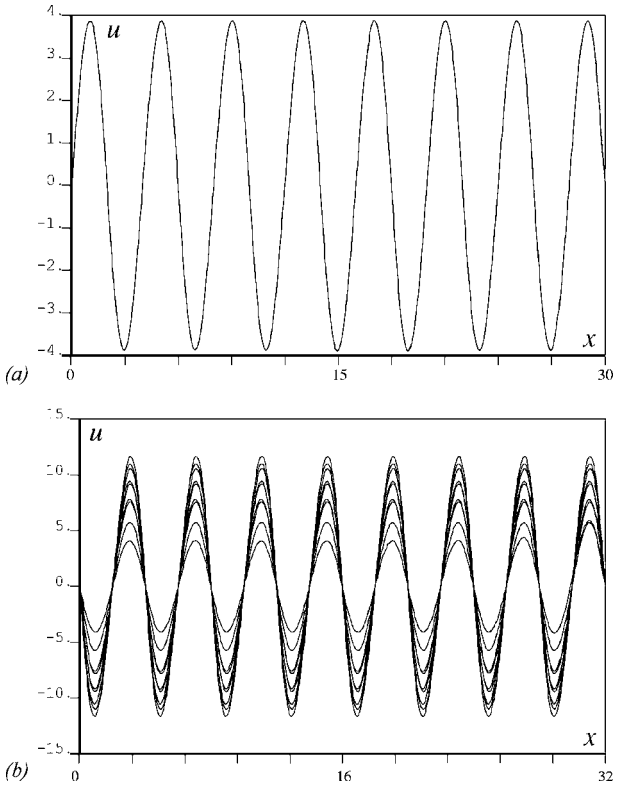

Fig. 12 Roll (cellular) solutions: (*a*) Solution E from Fig. 9; (*b*) a family of rolls for α between 2 and 7

solution. The curves intersect $\alpha=0$ at approximately regular intervals, separated by $\Delta L/2 \approx 4.42 \approx 2\pi/\sqrt{2}$. This value equals the wavelength of stationary oscillations about the trivial solution $u=0$, with wave number $k_s=\sqrt{2}$ (recall that the relevant part of the spectrum (3) for stationary solutions is $\lambda=0$). Thus we can propose an explanation for the discreteness and spacing of the fold curves in Fig. 13: We infer that the transition from one fold curve to the next at higher period L occurs, in the KS limit $\alpha=0$, via the insertion of two (by reversibility) complete oscillations with wave number k_s—asymptotically for large L—into the bubble. The number of bubble oscillations for $\alpha=0$ may thus serve to parametrize the fold curves. In summary, the transition from viscous shocks of the dKS equation to the KS equation is rather complicated, even in the context only of bifurcations of odd stationary periodic solutions. From the point of view of the observed PDE dynamics, however, it is equally important to investigate the *stability* of these stationary solutions.

5.3 Stability of Viscous Shocks. To supplement the existence results reported above, we discuss the stability of viscous shocks, and numerically compute boundaries of stability in a representative region in (α, L) parameter plane. To this end, we again use the continuation software AUTO, and adapt methods recently developed for the computation and continuation of spectra [26] to this fourth-order PDE (2). We emphasize that our computations cover only a small part of parameter space, but we expect that these reflect the general destabilization mechanisms when continuing viscous shocks to the KS limit $\alpha=0$. Our main results are plotted in Fig. 16, and we next describe our approach by continuation, referring to Ref. [26] for details.

We determine the stability of stationary solutions $u(x)$ via the spectrum of the linearization $\mathcal{L}(u)$ of Eq. (2) in a solution, as in Eq. (6); on an L-periodic domain, we write this operator as $\mathcal{L}_{\text{per}}(u): H^4_{\text{per}}([0,L]) \to L^2_{\text{per}}([0,L])$. Note that unlike in the B-S Eq. (8), $\mathcal{L}_{\text{per}}(u)$ is generally not self-adjoint (for $u \neq 0$), and its spectrum thus admits complex eigenvalues. In order to numerically continue selected eigenvalues of $\mathcal{L}_{\text{per}}(u)$ [26] it is helpful to view its spectrum as part of the spectrum of $\mathcal{L}(u)$ cast as an operator $\mathcal{L}_{\mathbb{R}}(u): H^4(\mathbb{R}) \to L^2(\mathbb{R})$. Recalling Eq. (7), we compute curves of this spectrum for fixed (α, L) by continuing solutions of the boundary value problem

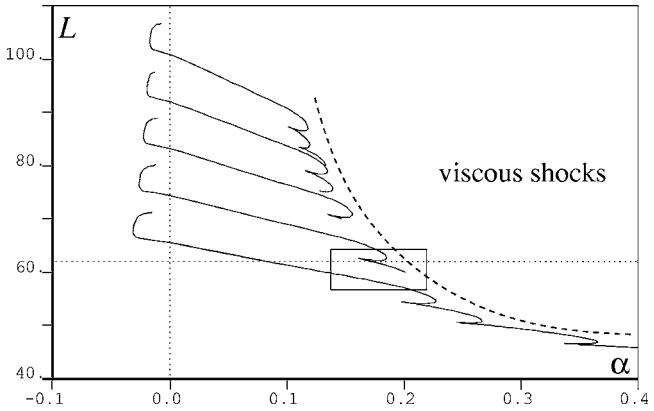

Fig. 13 Folds on different sheets of solutions in the (α, L) plane. The horizontal dotted line marks the slice shown in Fig. 14(*a*), and the box the range of Fig. 16(*a*). The sufficient existence criterion from Sec. 4 is sketched by the thick dotted line, but viscous shocks continue until the relevant fold curves to the left and below this curve.

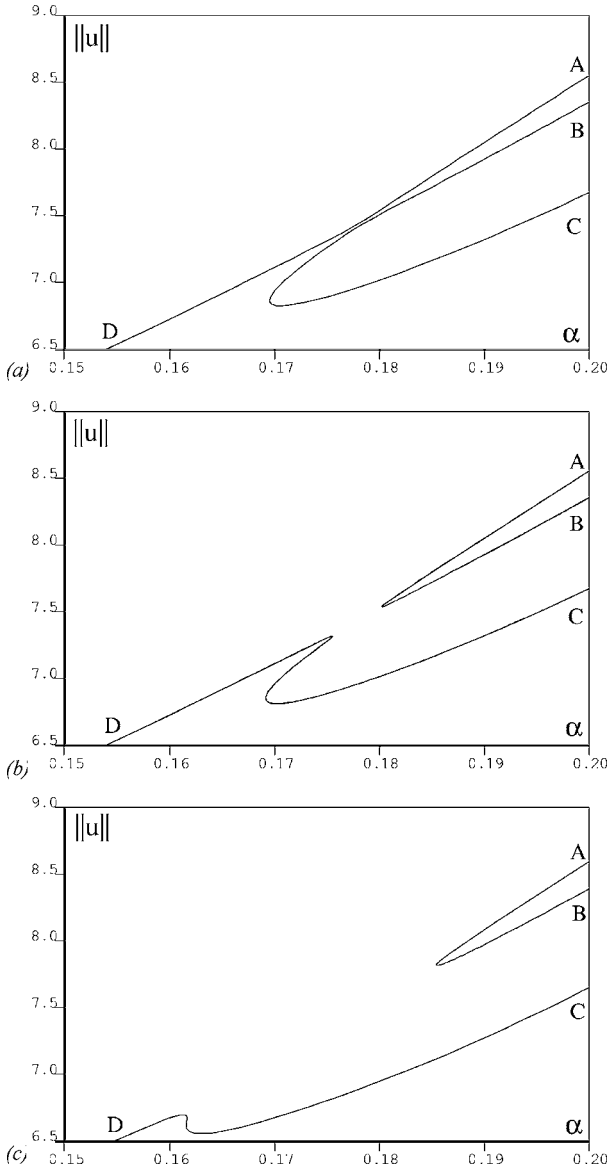

Fig. 14 Creation of a rip in the surface of viscous shocks at a fold point of folds: two sheets of solutions touch, and a pair of folds is created. (*a*) $L=62.20$: the upper branch A-D is a branch of viscous shocks, terminating in a fold to the left of D with smaller α; (*b*) $L=62.22$: two new folds created after the sheets of solutions touch and tear apart; the fold of viscous shocks is now the rightmost one connecting A and B; (*c*) $L=62.6$: cross section near the cusp point, at which two folds of flat shocks annihilate each other.

$$V_x = A(u,u_1,\lambda)V, \quad V(L) = e^{i\gamma}V(0) \tag{15}$$

in the parameter γ. To have full access to the points $(u(x),u_1(x))$, we solve Eq. (15) simultaneously with the nonlinear system (5) with reversible boundary conditions $u=u_{xx}=0$; periodic boundary conditions could also be implemented with appropriate modifications to break the reversible symmetry and fix the phase. For $\gamma \in 2\pi\mathbb{Z}$, Eq. (15) is precisely the eigenvalue problem for $\mathcal{L}_{\text{per}}(u)$, and its finite difference approximation was used to obtain initial conditions for the computations.

Figure 15 shows the result of one such computation, for $L=60$, $\alpha=0.15$, in which we plot the most unstable curves in the spectrum of $\mathcal{L}_{\mathbb{R}}(u)$; each of the isolated parts of this spectrum contains an eigenvalue of $\mathcal{L}_{\text{per}}(u)$ [26], so that for these parameters the viscous shock is unstable, with four complex conjugate pairs of eigenvalues with positive real parts.

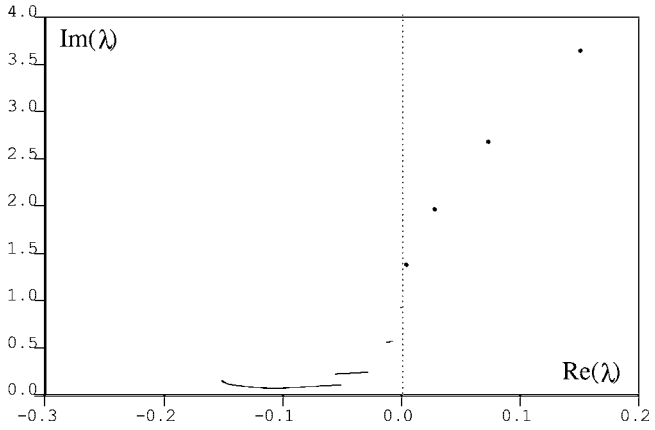

Fig. 15 Part of the essential spectrum of a viscous shock with $(\alpha,L)=(0.15,60)$ (only the spectrum in the upper half plane is needed, due to symmetry under complex conjugation). Bullets are used to enlarge the four unstable, extremely small closed isolated curves, each of which contains an eigenvalue of $\mathcal{L}_{\text{per}}(u)$.

Fixing $\gamma=0$ and L, we next continue the solution u together with an eigenfunction V and eigenvalue λ of $\mathcal{L}_{\text{per}}(u)$ in α, and thus locate the onset of instabilities of specific eigenvalues, where $\text{Re}(\lambda)=0$. By then fixing $\text{Re}(\lambda)=0$ in the boundary value problem (15), continuation in (α,L) yields the parameter curve along which this eigenvalue crosses the imaginary axis. Note that other eigenvalues may become unstable independently, though this is not the case here.

The spectrum plotted in Fig. 15 moves into the left half plane as α increases above $\alpha\approx 0.17$; this strict stability of the nontrivial eigenvalues implies exponential orbital stability of the underlying viscous shocks, as observed in the PDE simulations. Interpreting this for decreasing α, there is thus a Hopf bifurcation of viscous shocks for $L=60$, $\alpha\approx 0.17$. To locate the stability boundary for viscous shocks, we continue the Hopf bifurcation curves $\text{Re}(\lambda(\alpha,L))=0$ in the (α,L)-plane. In Fig. 16(*a*) we plot the resulting destabilization curve, which turns out to involve only one eigenvalue; here the thin lines are not relevant for viscous shocks, as they correspond to solutions on other solution sheets, reached via a fold or cusp. Combining the Hopf bifurcation curve of viscous shocks with the existence boundary consisting of fold curves and cusp points plotted in Fig. 13, we obtain part of the boundary of stable viscous shocks in the (α,L)-parameter plane as plotted in Fig. 16(*b*). In particular, the Hopf bifurcation curve connects two fold curves, and we conjecture that this structure persists throughout the (α,L) parameter plane. There is thus no connection of *stable* viscous shocks to the KS equation, as their region of existence is strictly bounded away from $\alpha=0$; rather, for decreasing $\alpha>0$ viscous shocks either cease to exist in a fold, or destabilize via Hopf bifurcations, as suggested by simulations of the PDE (2).

6 Discussion

The understanding of the origins of complex spatial and temporal behavior, such as observed and extensively studied in the Kuramoto-Sivashinsky equation, is advanced by the investigation of well-chosen limits, and to this end the destabilized KS Eq. (2) provides a particularly interesting model: for sufficiently large αL, the observed PDE dynamics appear almost gradient-like, with strong attraction to shock-like solutions, but these become unstable and cease to exist in the limit $\alpha\to 0$.

In the present work we have concentrated on the origins and bifurcations of the viscous shock solutions which occur for large αL. We have shown how to understand the emergence of viscous

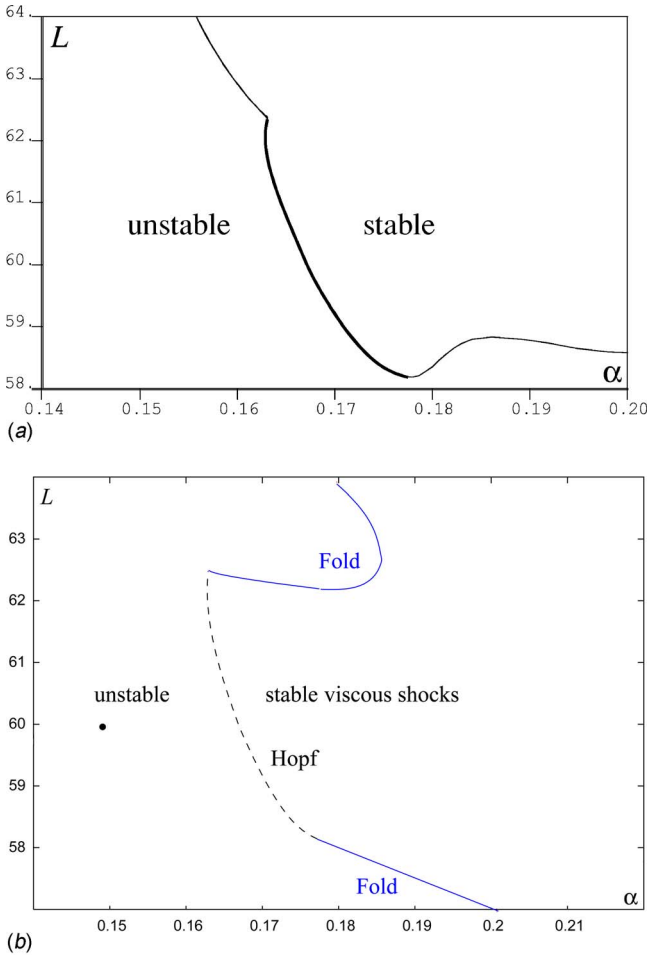

Fig. 16 (*a*) The onset of Hopf bifurcation in the (α, L) plane; only the thick line is relevant for viscous shocks. (*b*) The relevant part of (*a*) plotted together with fold curves from Fig. 13. The bullet denotes the location of the viscous shock used in Fig. 15.

shocks and related solutions geometrically in four-dimensional phase space: the invariant line due to the destabilizing term αu in Eq. (2) provides a reinjection mechanism that perturbs heteroclinic solutions to a rich family of periodic solutions with an extended linear region in their profile; for comparison, we have fully described this mechanism in the simpler second-order Burgers-Sivashinsky Eq. (8). The rigorous construction of these periodic solutions of a reversible four-dimensional dynamical system remains a challenge, however (due to the existence of a first integral, the corresponding study of stationary solutions for the KS Eq. (1) occurs in a simpler three-dimensional setting).

Using numerical continuation, we have explored the transition from viscous shocks to the KS limit, and even within the limited context of stationary, reversible solutions, the rich bifurcation structure and multitude of solutions are apparent. Of particular note is that the branches of viscous shocks are not stably connected to the KS limit $\alpha=0$ in (α, L) parameter space, either destabilizing via a Hopf bifurcation, or (in particular for fixed period L) ceasing to exist in a saddle-node bifurcation. To locate the Hopf bifurcations, we employed a recently developed approach to spectral computation via continuation, which allows the accurate detection of the onset of instability in a representative region of parameter space. The folds are due to the interaction of viscous shocks with related stationary solutions, and we computed several examples of solutions expected from the geometric analysis; a more systematic study should provide a fuller understanding of the solutions and bifurcations towards spatio-temporal chaos in the KS limit $\alpha \to 0$.

Acknowledgment

Much of this work was completed while J.R. was a PIMS postdoctoral fellow at Simon Fraser University and the University of British Columbia. J.R. thanks R.W. and Michael Ward for their support. We acknowledge helpful conversations with Björn Sandstede and J. F. Williams. This work was partially supported through an NSERC grant to R.W., and SPP 1095 of the German Research Foundation (J.R.).

References

[1] Cross, M., and Hohenberg, P., 1993, "Pattern Formation Outside of Equilibrium," Rev. Mod. Phys., **65**, pp. 851–1112.
[2] LaQuey, R., Mahajan, S., Rutherford, P., and Tang, W., 1975, "Nonlinear Saturation of the Trapped-Ion Mode," Phys. Rev. Lett., **34**, pp. 391–394.
[3] Sivashinsky, G., 1977, "Nonlinear Analysis of Hydrodynamic Instability in Laminar Flames—I. Derivation of Basic Equations," Acta Astron., **4**, pp. 1177–1206.
[4] Kuramoto, Y., and Tsuzuki, T., 1976, "Persistent Propagation of Concentration Waves in Dissipative Media far From Thermal Equilibrium," Prog. Theor. Phys., **55**, pp. 356–369.
[5] Misbah, C., and Valance, A., 1994, "Secondary Instabilities in the Stabilized Kuramoto-Sivashinsky Equation," Phys. Rev. E, **49**, pp. 166–183.
[6] Doelman, A., Sandstede, B., Scheel, A., and Schneider, G., 2005, "The Dynamics of Modulated Wave Trains," preprint.
[7] Wittenberg, R. W., and Holmes, P., 1999, "Scale and Space Localization in the Kuramoto-Sivashinsky Equation," Chaos, **9**, pp. 452–465.
[8] Wittenberg, R. W., and Holmes, P., 2002, "Spatially Localized Models of Extended Systems," Nonlinear Dyn., **25**, pp. 111–132.
[9] Michelson, D., 1986, "Steady Solutions of the Kuramoto-Sivashinsky Equation," Physica D, **19**, pp. 89–111.
[10] Kent, P., and Elgin, J., 1992, "Travelling-Waves of the Kuramoto-Sivashinsky Equation: Period-Multiplying Bifurcations," Nonlinearity, **5**, pp. 899–919.
[11] Jones, J., Troy, W. C., and MacGillivary, A. D., 1992, "Steady Solutions of the Kuramoto-Sivashinsky Equation for Small Wave Speed," J. Differ. Equations, **96**, pp. 28–55.
[12] Lamb, J. S. W., Teixeira, M.-A., and Webster, K. N., 2005, "Heteroclinic Bifurcations Near Hopf-Zero Bifurcation in Reversible Vector Fields in $\mathbb{R}^3$," J. Differ. Equations, **219**, pp. 78–115.
[13] Elgin, J. N., and Wu, X., 1996, "Stability of Cellular States of the Kuramoto-Sivashinsky Equation," SIAM J. Appl. Math., **56**, pp. 1621–1638.
[14] Hooper, A. P., and Grimshaw, R., 1988, "Travelling Wave Solutions of the Kuramoto-Sivashinsky Equation," Wave Motion, **10**, pp. 405–420.
[15] Adams, K. L., King, J. R., and Tew, R. H., 2003, "Beyond-All-Orders Effects in Multiple-Scales Asymptotics: Travelling-Wave Solutions to the Kuramoto-Sivashinsky Equation," J. Eng. Math., **45**, pp. 197–226.
[16] Wittenberg, R. W., 2002, "Dissipativity, Analyticity and Viscous Shocks in the (De)stabilized Kuramoto-Sivashinsky Equation," Phys. Lett. A, **300**, pp. 407–416.
[17] Chaté, H., and Manneville, P., 1987, "Transition to Turbulence via Spatiotemporal Intermittency," Phys. Rev. Lett., **58**, pp. 112–115.
[18] Goodman, J., 1994, "Stability of the Kuramoto-Sivashinsky and Related Systems," Commun. Pure Appl. Math., **47**, pp. 293–306.
[19] Bronski, J. C., and Gambill, T., 2005, "Uncertainty Estimates and L_2 Bounds for the Kuramoto-Sivashinsky Equation," preprint arXiv: math.AP/0508481.
[20] Giacomelli, L., and Otto, F., 2005, "New Bounds for the Kuramoto-Sivashinsky Equation," Commun. Pure Appl. Math., **58**, pp. 297–318.
[21] Devaney, R. L., 1976, "Reversible Diffeomorphisms and Flows," Trans. Am. Math. Soc., **218**, pp. 89–113.
[22] McCord, C. K., 1986, "Uniqueness of Connecting Orbits in the Equation $y^{(3)}=y^2-1$," J. Math. Anal. Appl., **114**, pp. 584–592.
[23] Fenichel, N., 1979, "Geometric Singular Perturbation Theory for Ordinary Differential Equations," J. Differ. Equations, **31**, pp. 53–98.
[24] Szmolyan, P., and Wechselberger, M., 2001, "Canards in R^3," J. Differ. Equations, **177**, pp. 419–453.
[25] Doedel, E., Paffenroth, R. C., Champneys, A. R., Fairgrieve, T. F., Kuznetsov, Y. A., Oldeman, B. E., Sandstede, B., and Wang, X., 2002, "AUTO2000: Continuation and Bifurcation Software for Ordinary Differential Equations (with HOMCONT)," Technical report, Concordia University, Montreal.
[26] Rademacher, J. D. M., Sandstede, B., and Scheel, A., 2005, "Computing Absolute and Essential Spectra using Continuation," IMA Preprint No. 2054, University of Minnesota, Minneapolis.